ACADEMIA ROMÂNĂ
Revue Roumaine de Chimie
http://web.icf.ro/rrch/

Rev. Roum. Chim.,
2014, *59*(2), 125-134

NANOSIZED Al_2O_3-TiO_2 OXIDE POWDER WITH ENHANCED POROSITY OBTAINED BY SOL-GEL METHOD

Tiberiu DASCALESCU, Ligia TODAN,* Adriana RUSU, Silviu PREDA, Cristian ANDRONESCU, Daniela C. CULITA, Cornel MUNTEANU and Maria ZAHARESCU*

"Ilie Murgulescu" Institute of Physical Chemistry, Roumanian Academy, 202 Splaiul Independentei, 060021 Bucharest, Roumania

Received January 13, 2014

Sol-gel process allows the synthesis of powders with a more elaborate structure and morphology, improving thus the reactivity of the synthesized material. Binary Oxide nanoparticles can have properties superior to those of the pure components. Oxides nanopowders in the Al_2O_3-TiO_2 system have been mainly used as raw materials for advanced polycrystalline Al_2TiO_5 ceramics synthesis. However, Al_2TiO_5 based powders have also other applications as for example in petroleum hydro-treatments or as potential adsorbents in the decontamination of chemical warfare agents. In the present work Al_2O_3-TiO_2 oxides were obtained by a sol-gel process and were characterized by thermogravimetric/differential thermal analysis, scanning electron microscopy, infrared spectroscopy, X-ray diffraction, BET specific surface area and porosity analysis. The obtained results were discussed comparatively with those obtained for the monocomponent oxides in order to establish new and better potential for their applications.

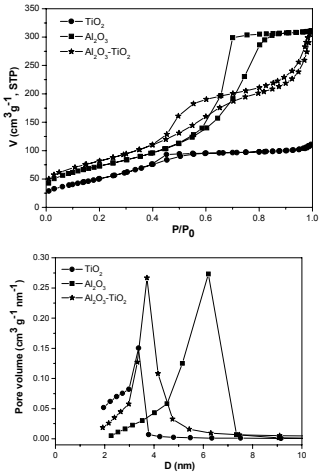

INTRODUCTION

Nanostructured materials, due to their small size and large specific surface areas, present novel properties not found in the bulk. They have been studied in order to find potential applications in various fields. Sol-gel process allows for the synthesis of powders with a more elaborate structure and morphology, improving thus the reactivity of the synthesized material

Titanium dioxide nanoparticles have shown excellent photocatalytic properties[1-5] but presented also interest for other applications as for example, chemical sensors[6] or solar cells.[7]

Alumina nanopowder has a widespread range of applications from catalysis[8,9] to optoelectronics[10,11] or biomedicine.[12,13]

Binary oxide nanoparticles can have superior properties to those of the pure components. Studies of the bicomponent compound consisting of these two oxides may provide data for improving the shortfalls of the individual oxides.[14,15] The investigation of titania-alumina nanopowders prepared by sol-gel method gave interesting results concerning the phases, morphology, particle size and composition of the samples. The most studies concerning the sol-gel preparation of the powders in the binary system were devoted to their use as precursor for the Al_2TiO_5 binary compound

* Corresponding authors: todanl@yahoo.com or mzaharescu2004@yahoo.com

formation[16,17] having applications for aeronautical and automotive purposes[17] or in orthopedic and dental implants.[19] However, tialite based powders have also other applications as for example in petroleum hydro-treatments[20] or as a potential adsorbent in the decontamination of chemical warfare agents.[21] For the two last applications the porosity of the powders is of great importance.

Nanosized TiO_2 powders were obtained most frequently by the titanium alkoxides hydrolysis[22-26] or by the precipitation of $TiCl_4$.[27] The sol-gel process is considered the most practical method among the various methods used to prepare nanopowders, because it confers the product a uniform pore size and high purity at low temperatures of preparation.

Al_2O_3 nanopowder is prepared frequently by the method developed by Yoldas.[28-30] Although important number of papers were published in the last time[31] using this method, other methods were also established, as precipitation from a $Al(NO_3)_3 \cdot 9H_2O$ solution with NH_4OH[32] or thermal treatment of a complex such as citrate salt.[33-35]

Binary powders offer the opportunity to manipulate the properties of the monocomponent systems to requirements. The Al_2O_3-TiO_2 binary powders were prepared mainly as precursors for tialite ceramics preparation. Studies have been undertaken on products obtained by the hydrolysis of aluminum and titanium alkoxides or of their inorganic salts. The mostly used method was the sol-gel co-gelation of the two oxides[36-39] but also precipitation of $AlCl_3$ and $TiCl_4$ with ammonia.[40]

In the present work, the sol-gel preparation and characterization of monocomponent Al_2O_3 and TiO_2 powders as well as of the binary powders in the AlO_3-TiO_2 system is illustrated. In addition, a comparative study of their structural and morphological properties is presented.

EXPERIMENTAL

Powders preparation

Powders were obtained in the Al_2O_3, TiO_2 monocomponent and Al_2O_3-TiO_2 bicomponent systems by sol-gel method. The composition of the precursor solutions and the experimental conditions are given in Table 1, based on the previous published results.[14,15]

In all cases the hydrolysis was realized with water excess. The oxide formation took place in un-catalyzed reaction mixtures. The obtained oxide powders were separated from the solution by filtration, washed, dried and then, according to the results of thermal analysis, they were thermally treated as follows: Al_2O_3 at 600°C, TiO_2 at 300°C, and Al_2O_3-TiO_2 at 450°C with 1h plateau and a heating rate of 1°C/min.

Powders characterization

The synthesized powders were characterized by thermogravimetric and thermodifferential analysis (DTA/TGA), scanning electron microscopy (SEM), Transform Fourier Infrared spectroscopy (FT-IR), X-ray diffraction (XRD) and specific surface area measurements.

Thermogravimetric and thermodifferential analysis (DTA/TGA) were performed using a Mettler Toledo TGA/SDTA851e equipment at a heating rate of 10°C/min, in air, with typically 20 mg sample.

The morphology of the samples were investigated by scanning electron microscopy (SEM) using a high-resolution microscope, FEI Quanta 3D FEG model, at low accelerating voltage (2-5 kV), in high vacuum mode with Everhart–Thornley secondary electron (SE) detector and backscatter electron detector. Samples preparation was minimal and consisted in immobilizing the material on a double-sided carbon tape, without coating.

FT-IR spectroscopic measurements were realized in transmission mode with a Nicolet Spectrometer 6700 FT-IR in the 400-4000 cm^{-1} range. The spectra were taken from thin transparent (~20 mg/cm^2) KBr pellets containing approximately 0.5% wt samples. Pellets were prepared by compacting and vacuum-pressing an intimate mixture obtained by grinding 1 mg of substance in 200 mg KBr.

Table 1

The initial composition of precursor solutions and the experimental conditions used for nanopowders synthesis

Sample	Reaction conditions			
	H_2O/Σprecursors	pH	Temperature of reaction (°C)	Time of reaction (h)
TiO_2[a]	5	5-6	25	0.5
Al_2O_3[b]	100	5-6	80	1.0
Al_2O_3-TiO_2	7.40	5-6	70	1.0

[a] precursor = $Ti(OC_2H_5)_4$;
[b] precursor = $Al(OiC_3H_7)_3$
[c] precursors = $Al(OiC_3H_7)_3$ and $Ti(O\text{-}iC_3H_7)_4$
[a and b] R = C_2H_5
[c] R = iC_3H_7
molar ratio Al_2O_3:TiO_2 = 1:1

Powder X-ray diffraction patterns (XRD) were recorded on a Rigaku Ultima IV apparatus, with CuK_α λ = 1.5406 Å radiation, in the 2θ=10-70^0 range, with a speed of 5^0/min and a 0.02 steps size, at 40 kV and 30 mA.

Nitrogen sorption isotherms at -196°C were recorded on a Micromeritics ASAP 2020 automated gas adsorption system. All the samples were outgassed at 350°C under vacuum prior to N_2 adsorption. Specific surface areas (S_{BET}) were calculated according to the Brunauer-Emmett-Teller (BET) equation using adsorption data at p/p0 = 0.05–0.20, while pore size distributions were derived from the desorption branch using the Barrett–Joyner–Halenda (BJH) model. Total pore volume was estimated from the amount adsorbed at the relative pressure of 0.99.

RESULTS AND DISCUSSION

In the experimental conditions presented above white nanometric powders were obtained. In order to establish the optimal thermal treatment required for elimination of the water and organic residues from the synthesis method of the obtained powders, their thermal behavior was studied by DTA/TGA measurements.

Thermal analysis

The thermal behavior of the individual as well as binary nanosized powders, in the 20–1000°C temperature range, is presented below (Figs. 1-3). In all cases the mass loss and the corresponding endothermic effects assigned to the evolution of adsorbed water and structural hydroxyls were observed.

In the case of the monocomponent powders the adsorbed water is evolved under 100^{o}C, being accompanied by an endothermal effect at 92^{o}C, in the case of TiO_2-based powder and 96^{o}C in the case of alumina-based powder.

The structural hydroxyls are eliminated in the 150-400^{o}C temperature range. In the case of alumina-based powder the process takes place in two steps. This thermal behaviour is characteristic for pseudo-boehmite decomposition.

The exothermal effect at 400^{o}C noticed in the case of the TiO_2 based powder, could be assigned to the anatase phase crystallization.

In the case of binary powder, one may notice that the DTA/TGA curves do not present the same thermal effects as the monocomponent ones. This observation allows concluding that the binary system is not a physical mixture of the individual oxides, but chemical bonds were realized during the sol-gel process between the TiO_2 and Al_2O_3 precursors.

The continuous weight loss with temperature and endothermal effect at low temperatures observed in the case of binary powder is characteristic for the homogeneous amorphous materials obtained by sol-gel method.

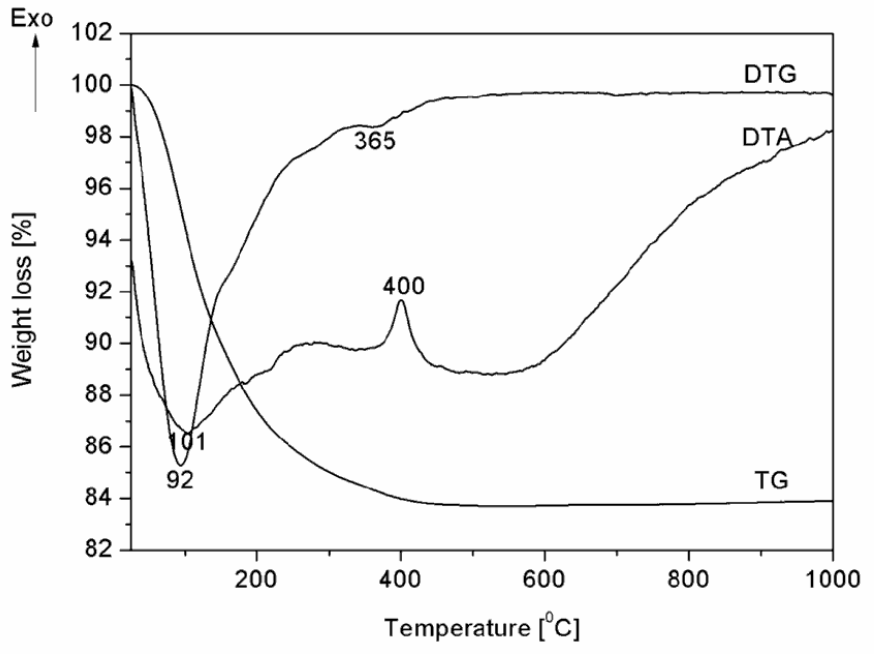

Fig. 1 – DTA/TGA curves of TiO_2 precursor powder.

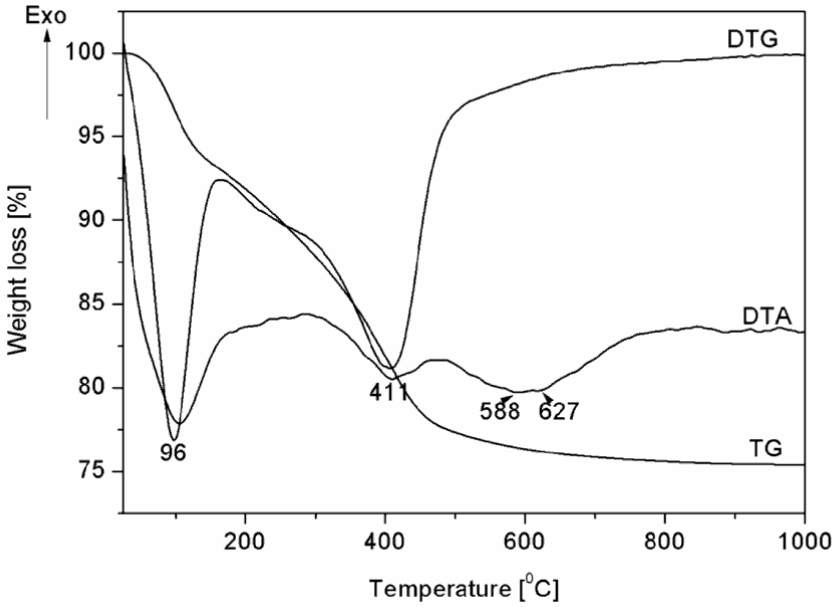

Fig. 2 – DTA/TGA curves of Al_2O_3 precursor powder.

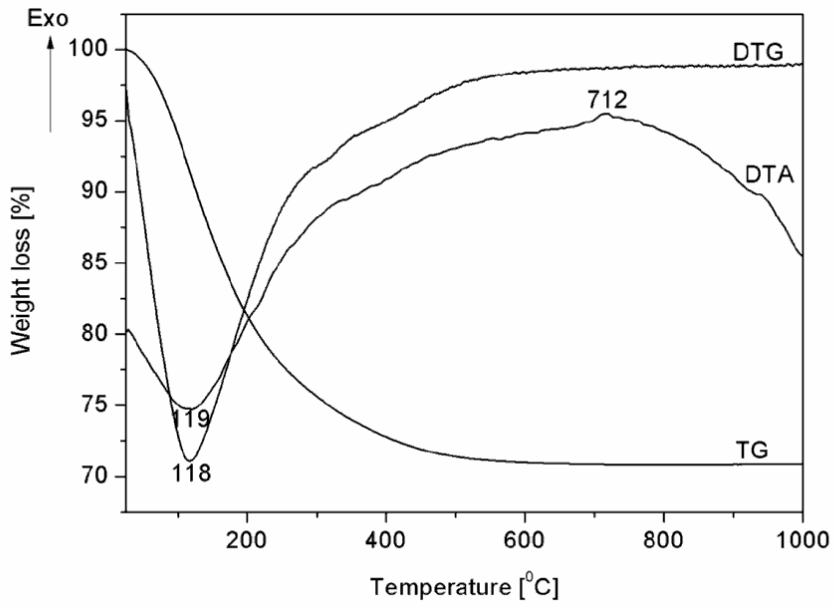

Fig. 3 – DTA/TGA curves of Al_2O_3-TiO_2 precursor powder.

SEM measurements

Powders obtained in the experimental conditions presented above, thermally treated at temperatures established by thermal analysis, namely Al_2O_3 at 600°C, TiO_2 at 300°C, and Al_2O_3-TiO_2 at 450°C, were nanometric and their morphology is shown in Figs. 4-6.

The morphology of the synthesized powders is different. In the case of monocomponent powders, the TiO_2 powder (Fig. 4) contains aggregates of particles with quasi-spherical shapes with diameter varying from approximately 0.3 to 1.3 microns. The aggregates are composed from nanoparticles of about 15 nm.

The SEM image of the Al_2O_3 powder presented in Fig. 5 shows the presence of very small particles (<10 nm) but with a very high tendency to agglomerate.

The binary powder, as resulted from the SEM image presented in Fig. 6, does not represent a mixture of the monocomponent ones, presenting a specific, different morphology as compared to the monocomponent ones.

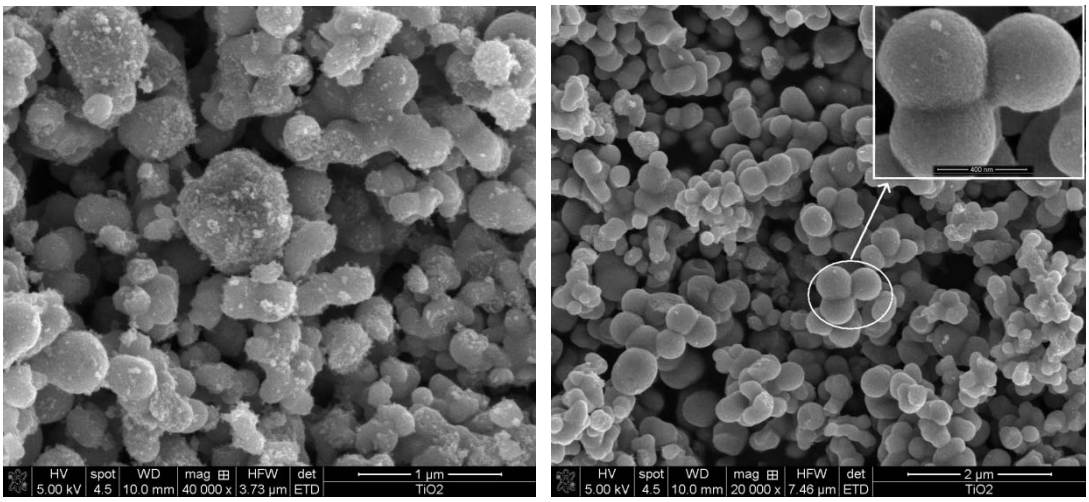

Fig. 4 – SEM image of TiO_2 powder.

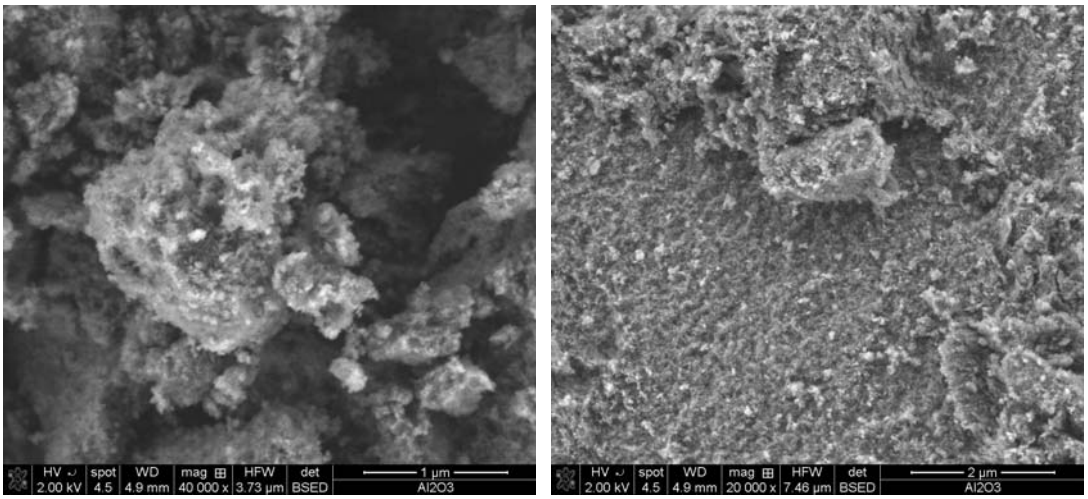

Fig. 5 – SEM image of Al_2O_3 powder.

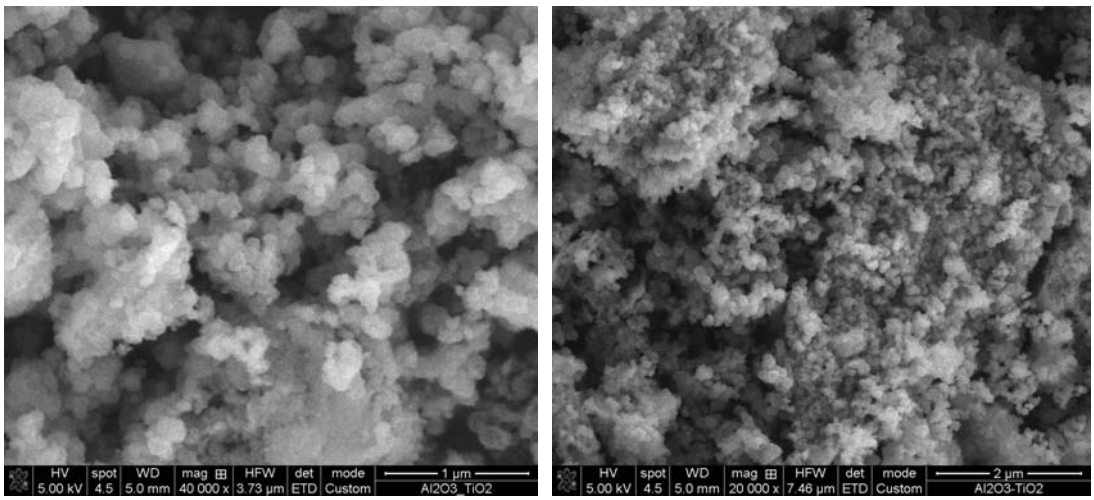

Fig. 6 – SEM image of Al_2O_3-TiO_2 powder.

FT-IR spectroscopy

The FT-IR spectra of the thermally treated powders are presented in Fig. 7. One may notice that in all cases besides the M-O-M vibration bands that are situated in the 400-1000 cm^{-1} range, characteristic vibration bands assigned to the presence of adsorbed water (1638 cm^{-1}), hydroxyls (3445 cm^{-1}) and organics adsorbed from the atmosphere (1410 cm^{-1} and 2928 and 2845 cm^{-1}) are noticed.

It is well known that some of the Ti–O and Al–O vibrations overlap in the spectra between 400 and 750 cm^{-1}. Generally, octahedral AlO_6 units are characterized by the presence of the stretching modes between 600 and 750 cm^{-1} and bending modes around 450 cm^{-1}. Tetrahedral coordinated Al–O shows peaks in the region of 750–850 cm^{-1}. [36,41] On the other hand, terminal Ti–O stretching vibration modes[36] are present in the spectra below 730 cm^{-1} and the band of a Ti–O–Ti bond of a titanium oxide network is detected at 640 cm^{-1}. [42] The FTIR spectrum of the binary gel powder range between 550 and 800 cm^{-1}. This is due to the overlapping of bands assigned to the tetrahedral coordination of Al and Ti in Al–O and Ti–O terminal bonds, respectively.

In addition, a new small band is detected at 583 cm^{-1} which can be assigned to hetero metal–oxygen bonds of –Ti–O–Al– .[43]

X-ray diffraction

The XRD patterns of the thermally treated powders are presented in the Figure 8.

XRD analysis was carried out in order to characterize the phase and crystal structure of the bulk samples. The polycrystalline diffractograms of the TiO_2, Al_2O_3,TiO_2-Al_2O_3 powder samples (Fig. 8) were compared to XRD patterns for anatase, γ-alumina and aluminium titanate structures from JCPDS references no. 78-2486, 10-0425 and 41-0258 in the International Centre for Diffraction Data (ICDD) database.

Average crystallite sizes of all the products were estimated using Scherrer equation: $D = k\lambda/(\beta\cos\theta)$, where λ is the employed X-ray wavelength, θ is the diffraction angle of the most intense diffraction peak, β is the full width at half maximum of the most intense diffraction peak (FWHM) and k is the Scherrer constant.[44] The Scherrer constant (k) in the formula accounts for the shape of the particle[45] and is generally taken to have the value 0.89.

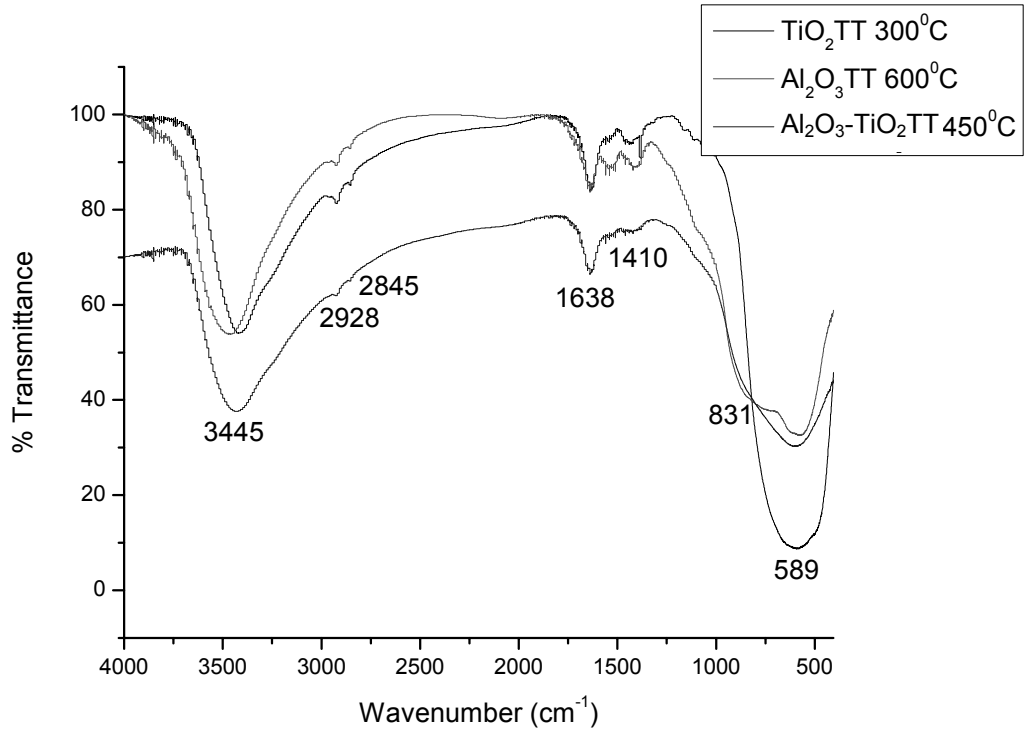

Fig. 7 – FT-IR spectra of the thermally treated monocomponent TiO_2, Al_2O_3, and binary TiO_2-Al_2O_3 nanopowders.

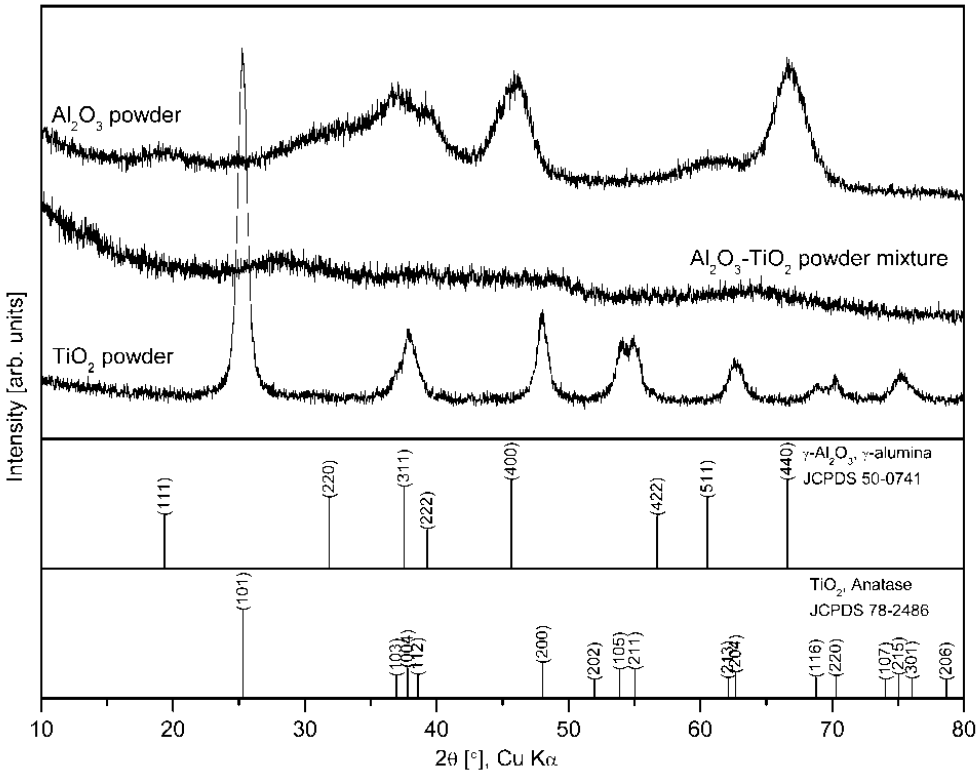

Fig. 8 – XRD pattern of thermally treated powders: a) TiO_2 at 300°C, b) Al_2O_3 at 600°C and c) TiO_2-Al_2O_3 at 450°C.

The diffractogram for TiO_2-Al_2O_3 powder corresponds to an amorphous structure.

The Al_2O_3 powder presents the reflections of (220), (311), (222), (400), (440) planes of the cubic structure of the γ-alumina phase, which is in agreement with the database standard and also the powder XRD studies of Lippens.[46] XRD pattern is characteristic of relatively poorly crystallized γ-alumina. The formation of γ-alumina is expected, because it is reported to be the most thermodynamically stable phase when the specific surface area of alumina is larger than 125 m^2/g, or when the crystallite size (particle diameter) is less than about 13 nm.

XRD pattern of TiO_2 powder sample is also shown in Fig. 8. XRD pattern exhibited strong diffraction lines at 25° and 48° indicating the phase pure anatase, as no rutile or brookite diffraction lines are detected. All diffraction lines are in good agreement with the standard pattern, mentioned above. It is well known that small crystallite size results in broadened diffraction patterns or diffused diffration lines in nanocrystals. These results suggested that the TiO_2 powder sample is composed of nanosized polycrystals.

Surface area and pore size distribution

The textural properties of the thermally treated pure TiO_2, Al_2O_3 oxides and TiO_2-Al_2O_3 oxide powders were compared through examining their nitrogen adsorption – desorption behaviors (Fig. 8). The BET surface area (S_{BET}), the cumulative pore volume (V_{total}) and the average pore diameters (D) of the samples are given in Table 2. As can be seen all samples exhibit typical IV type isotherms, characteristic of mesoporous materials, but with different hysteresis loops. The surface area of TiO_2-Al_2O_3 oxide (292.4 m^2/g) is higher than either TiO_2 (185.7 m^2/g) or Al_2O_3 oxides (262.3 m^2/g). The enhancement in the surface area of TiO_2-Al_2O_3 oxide confirms once again the ability of alumina to act as a morphology promoter for TiO_2.[47,48] The BJH pore-size analyses show a monomodal distribution of pores in a relatively narrow range 2 – 8 nm for all three samples with minimum at 3.38 nm for TiO_2, 3.71 nm for TiO_2-Al_2O_3 and 6.24 nm for Al_2O_3 (Fig. 9). The total pore volume of TiO_2-Al_2O_3 sample (0.47 cm^3/g) has the same value as in case of Al_2O_3 sample and is two times higher than that of TiO_2 sample.

The high values of the specific surface area determined for the synthesized sol-gel powders recommend them as good candidates for toxic organics adsorptions.

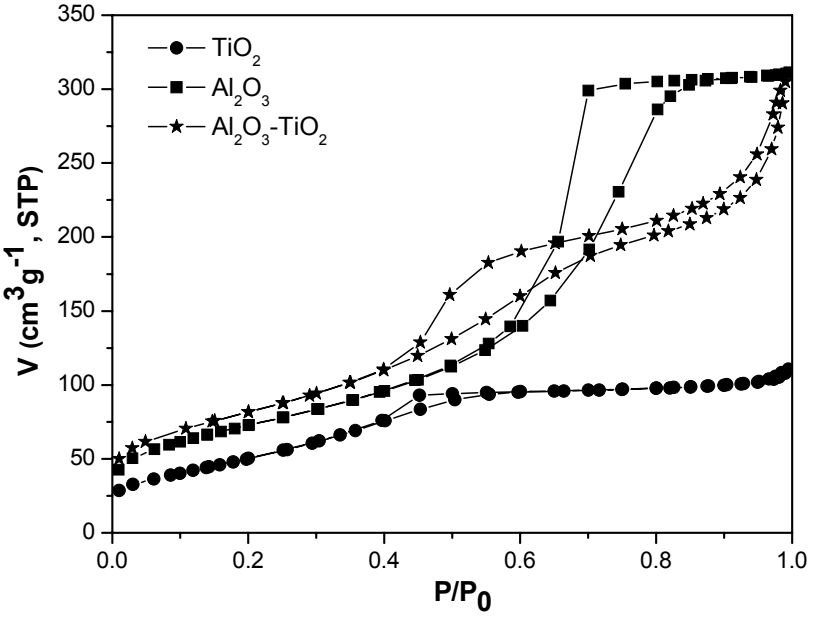

Fig. 9 – N_2 adsorption–desorption isotherms of the samples.

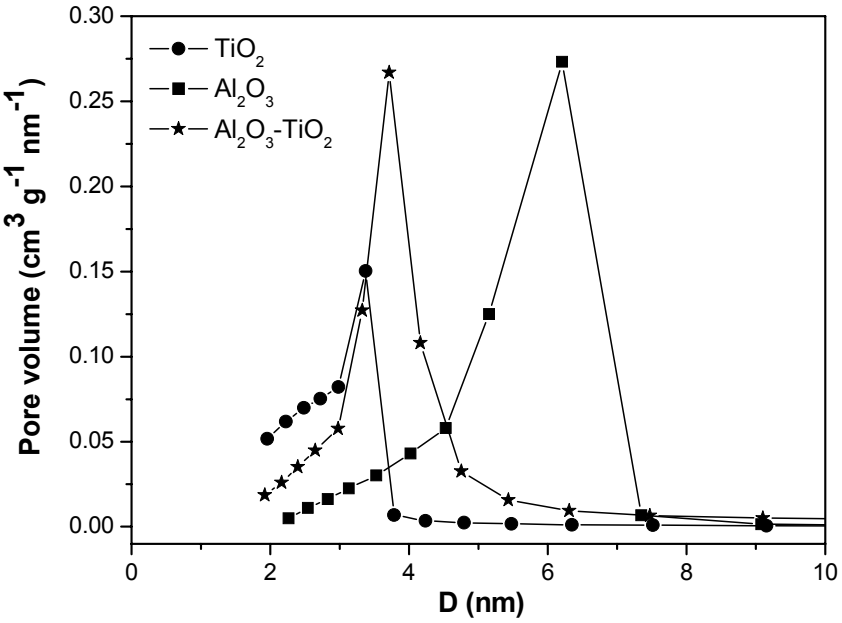

Fig. 9 – Pore size distribution of the samples.

Table 2

BET surface area (S_{BET}), total pore volume (V_{total}) and average pore diameter (D) of the thermally treated oxide powders

Sample	S_{BET} / m^2/g	V_{total} / cm^3/g	D / nm
TiO_2	185.7	0.16	3.22
Al_2O_3	262.3	0.47	5.44
Al_2O_3-TiO_2	292.4	0.47	5.28

CONCLUSIONS

TiO_2, Al_2O_3 and Al_2O_3-TiO_2 nanopowders were synthesized by sol-gel method in alcoholic medium.

The powders were characterized from the point of view of their structure, morphology, thermal stability and adsorption properties.

It was observed that TiO_2 powder thermally treated at 300°C presents high surface area (185.7 m^2/g) and has anatase structure.

In the case of Al_2O_3 powders, by thermal treatment γ-alumina structure was obtained and a higher surface area (262.3 m^2/g) as compared with that of the TiO_2 powder.

The Al_2O_3-TiO_2 powder thermally treated at 400°C remains amorphous and presents the highest specific surface area (292.4 m^2/g).

Investigations are underway in order to elucidate in more details the adsorption properties of the nanopowders in the Al_2O_3-TiO_2 system.

Aknowlegements: This paper was carried out within the research programme "Materials Science and Advanced Methods for Characterization" of the "Ilie Murgulescu" Institute of Physical Chemistry, financed by the Roumanian Academy. Support of the EU (ERDF) and Roumanian Government that allowed for acquisition of the research infrastructure under POS-CCE O 2.2.1 project INFRANANOCHEM - No. 19/01.03.2009 is gratefully acknowledged.

REFERENCES

1. A. Dodd, A. McKinley, T. Tsuzuki and M. Saunders, *J. Alloys Compd*., **2010**, *489*, L17-L21.
2. W. Wang, B. Gu, L. Liang, W. A. Hamilton and D. J. Wesolowski, *J. Phys. Chem. B*, **2004**, *108*, 14789-14792.
3 K. Yoo, H. Choi and D. D. Dionysiou, *Chem. Commun*., **2004**, 2000-2001.
4. C. Burda, Y. Lou, X. Chen, A.C.S. Samia and J. Stout, J.L. Gole, *Nano Letters*, **2003**, *3*, 1049-1051.
5. A. Mills, G. Hill, S. Bhopal, I. P. Parkin and S.A.J. O'Neil, *J. Photochem. Photobiol. A*, **2003**, *160*, 185-194.
6. L. Zheng, M. Xu and T. Xu, *Sens. Actuators*, **2000**, *66*, 28-30.
7. L. Zhang, A.J. Xie and Y.H. Shen, S.K. Li, *J. Alloys Compd*., **2010**, *505*, 579-583.
8. J. Cejka, *Appl. Catal. A*, **2003**, *254*, 327-338.
9. H. R. Zargar, M. R. Bayati, H. R. Rezaie, F. G. Fard, R. Molaei, S. Zanganeh and A. Kajbafvala, *J. Alloys Compd*., **2010**, *507*, 443-447.
10. Y. Teng, Y. Zhuang, G. Lin, J. Zhou, B. Zhu and J. Qiu, *J. Alloys Compd*., **2010**, *479*, 378-381.
11. S. Kurien, J. Mathew, S. Sebastian, S. N. Potty and K. C. George, *Mater. Chem. Phys*., **2006**, *98*, 470-476.
12. S. E. Kim, J. H. Lim, S. C. Lee, S.-C. Nam, H.-G. Kang and J. Choi, *Electrochim. Acta*, **2008**, *53*, 4846-4851.
13. S. Iftekar, J. Grins, G. Svensson, J. Loof, T. Jarmar, G.A. Botton, C.M. Andrei and H. J. Engqvist, *J. Eur. Ceram. Soc*., **2008**, *28*, 747-756.
14. M. Zaharescu, M. Crisan, D. Crisan, N. Dragan, A. Jitianu and M. Preda, *J. Eur. Ceram. Soc.*, **1998**, *18*, 1257-1264.
15. M. Crisan, A. Jitianu, M. Zaharescu, F. Mizukami and Shu-Ichi Niwa, *J. Dispers. Sci. Tech.*, **2003**, *24*, 129-144.
16. L. Stanciu, J. Groza, V. Kodash, M. Crişan and M. Zaharescu, *J. Amer. Ceram. Soc.*, **2001**, *84*, 983-985.
17. M. Preda, M. Crişan, A. Melinescu, S. Preda and M. Zaharescu, *Rev. Roum. Chim*., **2005**, *50*, 895-901.
18. F. Vaudry, S. Khodabandeh and M. E. Davis, *Chem. Mater.*, **1996**, *8*, 1451-1464.
19. V.R. Gonzalez, R. Zanella, G. de Angel and R. Gomeza, *J. Mol. Catal*., **2008**, *281*, 93-98.
20. H. K. Mishra, M. Stanciulescu, J.-P. Charland and J. F. Kelly, *Appl. Surf. Sci*., **2008**, *254*, 7098-7103.
21. T. M. Zima, N. I. Baklanova and N. Z. Lyakhov, *Inorg. Mater*., **2008**, *4*, 146-153.
22. M. Zaharescu, M. Crişan, L. Simionescu, D. Crişan and M. Gartner, *J. Sol-Gel Sci. Technol*., **1997**, *8*, 249-253.
23. M. Crişan, A. Brăileanu, M. Răileanu, D. Crişan, V. S. Teodorescu, R. Bîrjega, V. E. Marinescu, J. Madarász and G. Pokol, *J. Therm. Anal. Cal*., **2007**, *88*, 171-176.
24. M. Crişan, A. Brăileanu, M. Răileanu, M. Zaharescu, D. Crişan, N. Drăgan, M. Anastasescu, A. Ianculescu, I. Niţoi, V. E. Marinescu and S. M. Hodoroge, *J. Non-Cryst. Solids*, **2008**, *354*, 705-711.
25. M. Răileanu, M. Crişan, N. Drăgan, D. Crişan, A. Galtayries, A. Brăileanu, A. Ianculescu, V. S. Teodorescu, I. Niţoi and M. Anastasescu, *J. Sol-Gel Sci. Techn.*, **2009**, *51*, 315-329.
26. R. C. K. Kaminski, S. H. Pulcinelli, C.V. Santilli, F. Meneau, S. Blanchandin and V. Briois, *J . Eur. Ceram. Soc.*, **2010**, *30*, 193-198.
27. M. Kanna and S. Wongnawa, *Mat. Chem. Phys*., **2008**, *110*, 166-175.
28. B. E Yoldas, *Am. Ceram. Soc. Bull*., **1975**, *54*, 286-288.
29. B. E.Yoldas, *Am. Ceram. Soc.Bull*., **1975**, *54*, 289-290.
30. B. E. Yoldas, *J.Mater. Sci*., **1975**, *10*, 1856-1860.
31. M. Crişan, M. Zaharescu, V. Durga Kumari, M. Subrahmanyam, D. Crişan, N. Drăgan, M. Răileanu, M. Jitianu, A. Rusu, G. Sadanandam and J. K. Reddy, *Appl. Surf. Sci.*, **2011**, *258*, 448-455.
32. S. Jiansirisomboon and K. J. D. Mackenzie, *Mat. Res. Bull.*, **2006**, *41*, 791-803.
33. A. L. Ahmed, N. F. Idrus and M. R. Othman, *J. Membr. Sci.*, **2005**, *262*, 129-137.
34. J. Li, Y. Pan, C. Xiang, Q. Ge and J. Guo, *Ceram. Int.*, **2006**, *32*, 587-591.
35. M. Sharbatdaran, M. M. Amini and A. Majdabadi, *Mat. Lett.*, **2010**, *64*,503-505.
36. L.A. Stanciu, J. R. Groza, A. Jitianu and M. Zaharescu, *Mater. Manufacturing Proc.*, **2004**, *19*, 641-650.
37. M. Preda, A. Melinescu, M. Crişan, S. Preda and M. Zaharescu, *Rev. Roum. Chim*., **2006**, *51*, 509-515.
38. M. Sobhani, H. R. Rezaie and R. Naghizadeh, *J. Ma.*, *Procces. Technol.*, **2008**, *206*, 282-285.

39. Q.-C. Zhang, Q.-M. Ye, G. Li, J.-H. Lin, J.-F. Song, S.-H. Chang and J. Liu, *Mat. Lett.*, **2008**, *62*, 832-836.
40. M.A. Ahmed and M.F. Abdel-Messih, *J. Alloys Compd.*, **2011**, *509*, 2154-2159.
41. G. Urretavizcaya, A. L. Cavalieri, J. M. Porto Lopez, I. Sobrados and J. Sanz, *J. Mater.Synth. Process.*, 1998, *6*, 1-7.
42. M. J. Velasco, F. Rubio and J. L. Rubio, *Thermochim. Acta*, **1999**, *326*, 91-97.
43. S. Tursiloadi, H. Imai and H. Hirashima, *J. Non-Cryst. Solids*, **2004**, *350*, 271-276.
44. A. L. Patterson, *Phys.Rev.*, **1939**, *56*, 978-982.
45. H. Jensen, J. H. Pedersen, J. E. Jørgensen, J. Skov Pedersen, K. D. Joensen, S. B. Iversen and E. G. Søgaard, *J. Experim. Nanosci.*, **2006**, *1*, 355-373.
46. B. C. Lippens and J. H. De Boer, *Acta Crystall.*, **1964**, *17*, 1312-1321.
47. S. Sivakumar, C. P. Sibu, P. Mukundan, P. Krishna Pillai and K. G. K. Warrier, *Mat. Lett.*, **2004**, *58*, 2664– 2669.
48. A. Gutierrez-Alejandre, M. Trombetta, G. Busco and J. Ramirez, *Microporous Mat.*, **1997**, *12*, 79-91.